JOURNAL OF THEORETICAL
AND APPLIED MECHANICS
51, 2, pp. 313-325, Warsaw 2013

NUMERICAL CHARACTERIZATION OF AN AXISYMMETRIC LINED DUCT WITH FLOW USING THE MULTIMODAL SCATTERING MATRIX

Mohamed Taktak, Mohamed Ali Majdoub, Mohamed Haddar
University of Sfax, National School of Engineers of Sfax, Unit of Mechanics, Modelling and Production, Sfax, Tunisia
e-mail: mohamed.taktak@fss.rnu.tn

Mabrouk Bentahar
University of Technology of Compiègne, Roberval Laboratory UMR UTC-CNRS no. 6253, Compiègne Cedex, France

In this paper, the development of a numerical method to compute the multimodal scattering matrix of a lined duct in the presence of flow is presented. This method is based on the use of the convected Helmholtz equation and the addition of modal pressures at duct boundaries as additional degrees of freedom of the system. The boundary effects at the inlet and outlet of the finite waveguide are neglected. The choice of this matrix is justified by the fact that it represents an intrinsic characterization of a duct system. The validation of the proposed finite element is done by a comparison with the analytical formulation for simple cases of ducts. Then, the numerical coefficients of the scattering matrix of a lined duct and its acoustic power attenuation are computed for several flow velocities to evaluate the flow effect.

Key words: lined duct, scattering matrix, mean flow

1. Introduction

The characterization of the acoustic behavior of aircraft engines is an important tool used by engine designers to reduce the noise inside such systems and radiated from them. These engines are generally presented as a wave guide composed of an acoustic source and a series of a rigid wall and lined ducts. To characterize these wave guide systems, some specific matrices are used such as the mobility matrix as used by Pierce (1981), transfer matrix, see To and Doige (1979a,b), Lung and Doige (1983), Munjal (1987), Peat (1988) and Craggs (1989), reflection matrix presented in Akoum and Ville (1998) and Sitel *et al.* (2003), transmission matrix see Sitel *et al.* (2003) or scattering matrix see Abom (1991), Leroux *et al.* (2003), Bi *et al.* (2006) and Sitel *et al.* (2006) matrices. In a previous work, Taktak *et al.* (2010) developed the multimodal scattering matrix of a lined duct to characterize an axisymmetric rigid wall – lined – rigid wall duct simulating an aircraft engine without flow. In fact, this matrix represents an intrinsic characterization of the duct element independently of the upstream and downstream conditions: it depends only on acoustics and geometrical duct features and provides a complete description of the modal reflection, transmission and conversion of the duct element. This matrix is also used to evaluate the efficiency of the duct by computing its acoustic power attenuation as presented by Aurégan and Starobinski (1998) and Taktak *et al.* (2010). In that latter work, the scattering matrix was used to evaluate the efficiency of a lined duct and to characterize duct edges by calculation of its acoustic impedance without flow. But in a real engine the flow is present and has an important effect on the acoustic behavior of liners. For this rreason, a method based on the finite element method to compute the multimodal scattering matrix of a lined duct in the presence of a uniform flow with a Mach number smaller than unity is presented in this paper. This matrix is then used to characterize the acoustic performance of the studied duct by computing its acoustic power attenuation and to evaluate the flow effects on these parameters (scattering coefficients and acoustic attenuation).

In this paper, the studied problem is presented in Section 2. Then, the finite element method to compute the numerical multimodal scattering matrix with flow of a lined duct is presented in Section 3. Section 4 presents the computation of the acoustic power attenuation from the scattering matrix. Results of the proposed numerical method are presented and discussed in Section 5 to evaluate the flow effect.

2. Description of the physical problem

The studied duct is cylindrical. Figure 1 presents its symmetric part. It does not present a sudden section change but an impedance discontinuity caused by the liner which is supposed to be locally reacting is modeled by its acoustic impedance Z. Ω is the acoustic domain inside the duct. The edge of the studied duct is composed of four parts: the rigid wall duct part Γ_{WD}, the lined duct part Γ_{LD}, the left transversal boundary Γ_L and the right transversal boundary Γ_R. Γ_{WD}, Γ_{LR}, Γ_L and Γ_R are characterized respectively by their normal vectors $\mathbf{n}_{WD}$, $\mathbf{n}_{LD}$, $\mathbf{n}_L$ and $\mathbf{n}_R$. A uniform flow with a Mach number smaller than unity is present in this duct modeled by the vector $\mathbf{M}_0$ defined as

$$\mathbf{M}_0 = \Big(\frac{\mathbf{U}_0}{c}\Big) = \Big(\frac{U_0\mathbf{z}}{c}\Big) = M_0\mathbf{z} \tag{2.1}$$

where M_0 is the Mach number, U_0 is the flow velocity, c is the sound velocity and $\mathbf{z}$ is the duct axis. The objective of this work is the characterization of an industrial duct composed of a rigid wall and lined parts and the evaluation of its efficiency as well as the flow effect on the acoustic behavior of this duct. This is obtained by using the multimodal scattering matrix, from which the acoustic power attenuation is deduced. The methodology of numerical computation of this matrix as well as of the acoustic attenuation is presented in the next sections.

3. Computation of the multimodal scattering matrix

3.1. Definition of the scattering matrix

The scattering matrix $\mathbf{S}_{N\times N}$ of the duct element relates the outcoming pressure waves array $\mathbf{P}_{2N}^{out} = [P_{00}^{I-},\dots,P_{PQ}^{I-},P_{00}^{II+},\dots,P_{PQ}^{II+}]_N^{\mathrm{T}}$ to the incoming pressure waves array $\mathbf{P}_{2N}^{in} = [P_{00}^{I+},\dots,P_{PQ}^{I+},P_{00}^{II-},\dots,P_{PQ}^{II-}]_N^{\mathrm{T}}$ (Fig. 1) as follows, see Taktak *et al.* (2010)

$$\mathbf{P}_{2N}^{out} = \mathbf{S}_{2N\times 2N}\mathbf{P}_{2N}^{in} = \begin{bmatrix} \mathbf{R}_{N\times N}^{+} & \mathbf{T}_{N\times N}^{+} \\ \mathbf{T}_{N\times N}^{-} & \mathbf{R}_{N\times N}^{-} \end{bmatrix}_{2N\times 2N} \mathbf{P}_{2N}^{in} \tag{3.1}$$

where P_{mn}^{I+} and P_{mn}^{I-} are the modal pressure coefficients associated to the (m,n) mode traveling, respectively, in the positive and the negative direction in region I, P_{mn}^{II+} and P_{mn}^{II-} are respectively the modal pressure coefficients associated to the (m,n) mode traveling, respectively, in the positive and the negative direction in region II (Fig. 1). m and n are, respectively, the azimuthal and the radial mode numbers. N is the number of modes in both cross sections, P and Q are, respectively, the angular and radial wave numbers associated to the N-th propagating mode ($m \leqslant P$ and $n \leqslant Q$).

3.2. Governing equations

The studied duct is axisymmetric. The boundary effects at the inlet and outlet of the duct are neglected. The acoustic pressure p in the duct is the solution of the system containing

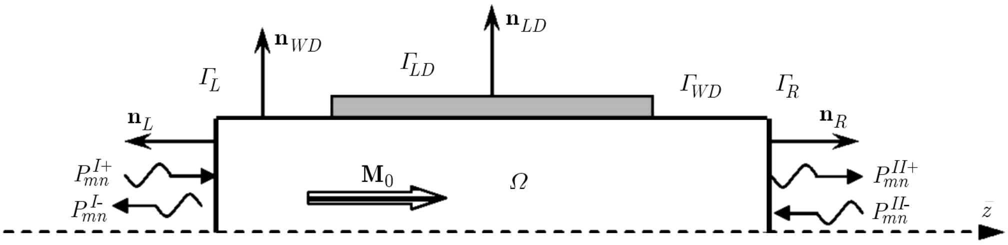

Fig. 1. Schematic of the theoretical model for the computation of the multimodal scattering matrix

the convected Helmholtz equation with boundaries conditions at Γ_{WD} (rigid wall duct part) and Γ_{LD} (lined duct part)

$$\begin{aligned}
&\Delta p + k^2 p + \frac{2\mathrm{i}\omega}{c}(\mathbf{M}_0\cdot\nabla p) - \mathbf{M}_0\cdot\nabla(\mathbf{M}_0\cdot\nabla p) = 0 && (\Omega)\\
&Z\frac{\partial p}{\partial n_{LD}} = \frac{\rho_0}{\mathrm{i}\omega}\Big(-\mathrm{i}\omega + U_0\frac{\partial}{\partial z}\Big)^2(p) && (\Gamma_{LD})\\
&\frac{\partial p}{\partial n_{WD}} = 0 && (\Gamma_{WD})
\end{aligned} \tag{3.2}$$

where Δ is the Laplacian operator; k is the total wave number, ρ_0 is the density and ω is the pulsation. $\nabla = \langle \partial/\partial r, \mathrm{i}m/r, \partial/\partial z\rangle^{\mathrm{T}}$ is the modified gradient for axisymmetric problems. χ_{mn} is the n-th root satisfying the radial hard-boundary condition on the rigid wall of the main duct. The acoustic pressure fields at the left section Γ_L and the right section Γ_R (Fig. 1) are given as follows

$$\begin{aligned}
p^L &= \sum_n^{N_r}\Big(P_{mn}^{I+}\mathrm{e}^{\mathrm{i}k_{mn}^+(z-z_L)} + P_{mn}^{I-}\mathrm{e}^{\mathrm{i}k_{mn}^-(z-z_L)}\Big)J_m\Big(\frac{\chi_{mn}}{a}r\Big)\\
p^R &= \sum_n^{N_r}\Big(P_{mn}^{II+}\mathrm{e}^{\mathrm{i}k_{mn}^+(z-z_R)} + P_{mn}^{II-}\mathrm{e}^{\mathrm{i}k_{mn}^-(z-z_R)}\Big)J_m\Big(\frac{\chi_{mn}}{a}r\Big)
\end{aligned} \tag{3.3}$$

with N_r being the number of radial modes. z_L and z_R are, respectively, the axial position of the left and right boundaries, J_m is the Bessel function of the first kind of the order m, a is the duct radius, r is the radial variable. $k_{mn}^{\pm}$ are the axial wave numbers associated with the (m,n) mode and defined as

$$k_{mn}^{\pm} = \frac{-M_0 k \pm \sqrt{k^2 - (1-M_0^2)k_t^2}}{1-M_0^2} \tag{3.4}$$

where k_t is the transverse wave number. The sign "+" means that the axial wave number is calculated in the same direction of the flow, the sign "−" means that the axial wave number is calculated in the opposite direction of the flow.

3.3. Variational formulation

To solve problem (3.2), the finite element method is used. The weak variational formulation of this problem is written as follows

$$\begin{aligned}
\Pi = &\int_\Omega -(\nabla q\cdot\nabla p)r\,d\Omega + \frac{1}{c^2}\int_\Omega(\mathrm{i}\omega q + \mathbf{U}_0\cdot\nabla q)(-\mathrm{i}\omega p + \mathbf{U}_0\cdot\nabla p)r\,d\Omega\\
&+ \int_{\cup\Gamma_i}\Big[q\frac{\partial p}{\partial n_i} - \frac{1}{c^2}\mathbf{U}_0\cdot\mathbf{n}_i q\Big(-\mathrm{i}\omega + U_0\frac{\partial}{\partial n_i}\Big)(p)r\,d\Gamma_i = 0
\end{aligned} \tag{3.5}$$

where p and q are, respectively, the acoustic pressure in the duct and the test function. $d\Omega = dr\,dz$ is the surface element. $\cup\Gamma_i$ present the whole boundaries ($i = LD$ – lined part, $i = L$ – left, $i = R$ – right). The third integral includes boundary conditions. This integral is composed of three parts:

— Lined part Γ_{LD}

$$\begin{aligned}\int\limits_{\Gamma_{LD}} \Big[q\frac{\partial p}{\partial n_{LD}} - \frac{1}{c^2}\mathbf{U}_0\cdot\mathbf{n}_{LD}q\Big(-\mathrm{i}\omega + U_0\frac{\partial}{\partial n_{LD}}\Big)(p)\Big]r\,d\Gamma_{LD} &= -\rho_0\omega^2\int\limits_{\Gamma_{LD}} q\frac{p}{\mathrm{i}\omega Z}r\,d\Gamma_{LD}\\ &- 2\mathrm{i}\omega\rho_0U_0\int\limits_{\Gamma_{LD}} q\frac{\partial}{\partial z}\Big(\frac{p}{\mathrm{i}\omega Z}\Big)r\,d\Gamma_{LD} - \rho_0U_0^2\int\limits_{\Gamma_{LD}}\frac{\partial q}{\partial z}\frac{\partial}{\partial z}\Big(\frac{p}{\mathrm{i}\omega Z}\Big)r\,d\Gamma_{LD}\\ &+ \rho_0U_0^2\Big[rq\frac{\partial}{\partial z}\Big(\frac{p}{\mathrm{i}\omega Z}\Big)\Big]^{L_{LD}}\end{aligned} \tag{3.6}$$

with LLD being the lined part length.

— Left boundary Γ_L

$$\begin{aligned}&\int\limits_{\Gamma_L}\Big[q\frac{\partial p}{\partial n_L} - \frac{1}{c^2}\mathbf{U}_0\cdot\mathbf{n}_Lq\Big(-\mathrm{i}\omega + U_0\frac{\partial}{\partial n_L}\Big)(p)\Big]r\,d\Gamma_L\\ &= \sum_{n=1}^{N_r}\mathrm{i}n_L\Big[(1+M_0^2)(k_{mn}^+P_{mn}^{I+} + k_{mn}^-P_{mn}^{I-}) - kM_0(P_{mn}^{I+} + P_{mn}^{I-})\Big]\int\limits_{\Gamma_L} qJ_m\Big(\frac{\chi_{mn}}{a}r\Big)r\,d\Gamma_L\end{aligned} \tag{3.7}$$

— Right boundary Γ_R

$$\begin{aligned}&\int\limits_{\Gamma_R}\Big[q\frac{\partial p}{\partial n_R} - \frac{1}{c^2}\mathbf{U}_0\cdot\mathbf{n}_Rq\Big(-\mathrm{i}\omega + U_0\frac{\partial}{\partial n_R}\Big)(p)\Big]r\,d\Gamma_R\\ &= \sum_{n=1}^{N_r}\mathrm{i}n_R\Big[(1+M_0^2)(k_{mn}^+P_{mn}^{II+} + k_{mn}^-P_{mn}^{II-}) - kM_0(P_{mn}^{II+} + P_{mn}^{II-})\Big]\int\limits_{\Gamma_R} qJ_m\Big(\frac{\chi_{mn}}{a}r\Big)r\,d\Gamma_R\end{aligned} \tag{3.8}$$

The use of modal decomposition at the boundaries Γ_L and Γ_R in Eq. (3.3) introduces the modal pressures as additional degrees of freedom of the model. It is necessary to complete Eqs. (3.5), (3.6) and (3.7) with more equations to obtain a well posed problem. This is done by supposing that pressures at Γ_L and Γ_R can be obtained by the projection of the acoustic field over the eigenfunctions of the rigid wall duct

$$\begin{aligned}\int\limits_{\Gamma_L} pJ_m\Big(\frac{\chi_{mn}}{a}r\Big)\,d\Gamma_L &= (P_{mn}^{I+} + P_{mn}^{I-})\int\limits_{\Gamma_L} J_m\Big(\frac{\chi_{mn}}{a}r\Big)^2 r\,d\Gamma_L\\ \int\limits_{\Gamma_R} pJ_m\Big(\frac{\chi_{mn}}{a}r\Big)\,d\Gamma_R &= (P_{mn}^{II+} + P_{mn}^{II-})\int\limits_{\Gamma_R} J_m\Big(\frac{\chi_{mn}}{a}r\Big)^2 r\,d\Gamma_R\end{aligned} \tag{3.9}$$

3.4. Finite element discritization

To solve the proposed problem, the domain (Ω) is discretized with triangular finite elements while the edges are meshed by two node finite elements. The computation of integrals of Eq. (3.4) is made by the summation over the finite elements number of elementary integrals (Dhatt and Touzout, 1989)

$$
\begin{aligned}
I_{e1} &= \int\limits_{\Omega_e} -(\nabla q \cdot \nabla p) r \, d\Omega_e + \frac{1}{c^2} \int\limits_{\Omega_e} (\mathrm{i}\omega q + \mathbf{U}_0 \cdot \nabla q)(-\mathrm{i}\omega p + \mathbf{U}_0 \cdot \nabla p) r \, d\Omega_e \\
I_{e2} &= -\rho_0 \omega^2 \int\limits_{\Gamma_e} q \frac{p}{\mathrm{i}\omega Z} r \, d\Gamma_e - 2\mathrm{i}\omega \rho_0 M_0 \int\limits_{\Gamma_e} q \frac{\partial}{\partial z}\Big(\frac{p}{\mathrm{i}\omega Z}\Big) r \, d\Gamma_e - \rho_0 M_0^2 \int\limits_{\Gamma_e} \frac{\partial q}{\partial z} \frac{\partial}{\partial z}\Big(\frac{p}{\mathrm{i}\omega Z}\Big) r \, d\Gamma_e \\
I_{e3} &= \rho_0 M_0^2 \Big[rq \frac{\partial}{\partial z}\Big(\frac{p}{\mathrm{i}\omega Z}\Big)\Big]^{L_{LD}} \\
I_{e4} &= \sum_{n=1}^{N_r} \mathrm{i} n_L \Big[(1+M_0^2)(k_{mn}^+ P_{mn}^{I+} + k_{mn}^- P_{mn}^{I-}) - k M_0 (P_{mn}^{I+} + P_{mn}^{I-})\Big] \int\limits_{\Gamma_e} q J_m \Big(\frac{\chi_{mn}}{a} r\Big) r \, d\Gamma_e \\
I_{e5} &= \sum_{n=1}^{N_r} \mathrm{i} n_R \Big[(1+M_0^2)(k_{mn}^+ P_{mn}^{II+} + k_{mn}^- P_{mn}^{II-}) - k M_0 (P_{mn}^{II+} + P_{mn}^{II-})\Big] \int\limits_{\Gamma_e} q J_m \Big(\frac{\chi_{mn}}{a} r\Big) r \, d\Gamma_e
\end{aligned}
\tag{3.10}
$$

The computation of integrals (3.9) is obtained by the summation over the finite elements number of elementary integrals

$$
\begin{aligned}
I_{e6} &= \int\limits_{\Gamma_e} p J_m \Big(\frac{\chi_{mn}}{a} r\Big) r \, d\Gamma_e - (P_{mn}^{I+} + P_{mn}^{I-}) \int\limits_{\Gamma_e} J_m \Big(\frac{\chi_{mn}}{a} r\Big)^2 r \, d\Gamma_e \\
I_{e7} &= \int\limits_{\Gamma_e} p J_m \Big(\frac{\chi_{mn}}{a} r\Big) r \, d\Gamma_e - (P_{mn}^{II+} + P_{mn}^{II-}) \int\limits_{\Gamma_e} J_m \Big(\frac{\chi_{mn}}{a} r\Big)^2 r \, d\Gamma_e
\end{aligned}
\tag{3.11}
$$

where Ω_e and Γ_e are, respectively, the elementary triangular and two-node finite elements.

3.4.1. Elementary computation of the triangular finite element

For the triangular finite element composed of three nodes, the integral I_{e1} is written as follows

$$
\begin{aligned}
I_{e1} &= [q_1, q_2, q_3](\mathbf{K}_e)_1 [p_1, p_2, p_3]^{\mathrm{T}} \\
(\mathbf{K}_e)_1 &= \int\limits_{\Omega_{ref}} -(\nabla q \cdot \nabla p^{\mathrm{T}}) \det \mathbf{j} \, r \, d\xi \, d\eta \\
&\quad + \int\limits_{\Omega_{ref}} \left(\frac{\mathrm{i}\omega}{c} \begin{Bmatrix} N_1' \\ N_2' \\ N_3' \end{Bmatrix} + \mathbf{U}_0 \cdot \nabla q \right) \Big(-\frac{\mathrm{i}\omega}{c} [N_1', N_2', N_3'] + \mathbf{U}_0 \cdot \nabla p \Big) \det \mathbf{j} \, r \, d\xi \, d\eta
\end{aligned}
\tag{3.12}
$$

where $p_i = 1, 2, 3$ and $q_i = 1, 2, 3$ are, respectively, nodal acoustic pressures and nodal test functions of the triangular finite element. $\mathbf{j}$ is the inverse matrix of the Jacobian matrix $\mathbf{J}$ of the transformation from the reference element to the real base and $N_1'(\xi, \eta)$, $N_2'(\xi, \eta)$ and $N_3'(\xi, \eta)$ are the interpolation functions of the triangular element (Dhatt and Touzout, 1989)

$$
N_1'(\xi, \eta) = 1 - \xi - \eta \qquad N_2'(\xi, \eta) = \xi \qquad N_3'(\xi, \eta) = \eta \tag{3.13}
$$

The integration of integral $(3.12)_2$ is made using the numerical Gauss integration method, see Dhatt and Touzout (1989). Finally, the global corresponding matrix is

$$
\mathbf{K}_1 = \sum_{1}^{NelT} (\mathbf{K}_e)_1 \tag{3.14}
$$

where $NelT$ is the number of triangular finite elements.

3.4.2. Elementary computations of the two node finite element

For the two-node finite element belonging to the lined part of the duct composed of two nodes, I_{e2} and I_{e3} are computed as follows

$$
\begin{aligned}
I_{e2} &= [q_1, q_2](\mathbf{K}_e)_2 \begin{Bmatrix} p_1 \\ p_2 \end{Bmatrix} \qquad (\mathbf{K}_e)_2 = (\mathbf{K}_e)_{21} + (\mathbf{K}_e)_{22} + (\mathbf{K}_e)_{23} \\
(\mathbf{K}_e)_{21} &= \rho_0 \mathrm{i}\omega \int\limits_{-1}^{1} \begin{Bmatrix} N_1 \\ N_2 \end{Bmatrix} [N_1, N_2] \frac{[N_1, N_2]}{[Z_1, Z_2] \begin{Bmatrix} N_1 \\ N_2 \end{Bmatrix}} \frac{L_e}{2} r \, d\xi \\
(\mathbf{K}_e)_{22} &= -2\rho_0 U_0 \int\limits_{-1}^{1} \begin{Bmatrix} N_1 \\ N_2 \end{Bmatrix} \left(\frac{\frac{2}{L_e}[-1/2, 1/2]}{[Z_1, Z_2] \begin{Bmatrix} N_1 \\ N_2 \end{Bmatrix}} - [N_1, N_2] \frac{\frac{2}{L_e}[Z_1, Z_2] \begin{Bmatrix} -1/2 \\ 1/2 \end{Bmatrix}}{\left([Z_1, Z_2] \begin{Bmatrix} N_1 \\ N_2 \end{Bmatrix} \right)^2} \right) \frac{L_e}{2} r \, d\xi \\
(\mathbf{K}_e)_{23} &= \frac{\rho_0 U_0^2}{\mathrm{i}\omega} \int\limits_{-1}^{1} \frac{2}{L_e} \begin{Bmatrix} -1/2 \\ 1/2 \end{Bmatrix} \left(\frac{\frac{2}{L_e}[-1/2, 1/2]}{[Z_1, Z_2] \begin{Bmatrix} N_1 \\ N_2 \end{Bmatrix}} - [N_1, N_2] \frac{\frac{2}{L_e}[Z_1, Z_2] \begin{Bmatrix} -1/2 \\ 1/2 \end{Bmatrix}}{\left([Z_1, Z_2] \begin{Bmatrix} N_1 \\ N_2 \end{Bmatrix} \right)^2} \right) \frac{L_e}{2} r \, d\xi
\end{aligned}
\tag{3.15}
$$

where $p_i = 1, 2$ and $q_i = 1, 2$ are, respectively, nodal acoustic pressures and nodal test functions of the two-node finite element. Z_1 and Z_2 are the acoustic impedance of each node of the two-node finite element. L_e is the finite element length, $N_1(\xi)$ and $N_2(\xi)$ are the interpolation functions of the two-node finite element defined by Dhatt and Touzout (1989)

$$
N_1(\xi, \eta) = \frac{1 - \xi}{2} \qquad N_2(\xi) = \frac{1 + \xi}{2} \tag{3.16}
$$

The computation of I_{e3} is done for the two-node finite elements on the lined part extremities in which the first node of the first finite element of this part and the second node of the last finite element of the lined part are used

$$
\begin{aligned}
I_{e3} &= [q_1, q_2](\mathbf{K}_e)_{3Z2} \begin{Bmatrix} p_1 \\ p_2 \end{Bmatrix} - [q_1, q_2](\mathbf{K}_e)_{3Z1} \begin{Bmatrix} p_1 \\ p_2 \end{Bmatrix} \\
(\mathbf{K}_e)_{3Z2} &= \frac{\rho_0 U_0^2}{\mathrm{i}\omega} \frac{2}{L_e} \begin{Bmatrix} 0 \\ 1 \end{Bmatrix} \left(\frac{[-1/2, 1/2]}{[Z_1, Z_2] \begin{Bmatrix} 0 \\ 1 \end{Bmatrix}} - [0, 1] \frac{[Z_1, Z_2] \begin{Bmatrix} -1/2 \\ 1/2 \end{Bmatrix}}{\left([Z_1, Z_2] \begin{Bmatrix} 0 \\ 1 \end{Bmatrix} \right)^2} \right) [r_1, r_2] \begin{Bmatrix} 0 \\ 1 \end{Bmatrix} \\
(\mathbf{K}_e)_{3Z1} &= \frac{\rho_0 U_0^2}{\mathrm{i}\omega} \frac{2}{L_e} \begin{Bmatrix} 1 \\ 0 \end{Bmatrix} \left(\frac{[-1/2, 1/2]}{[Z_1, Z_2] \begin{Bmatrix} 1 \\ 0 \end{Bmatrix}} - [1, 0] \frac{[Z_1, Z_2] \begin{Bmatrix} -1/2 \\ 1/2 \end{Bmatrix}}{\left([Z_1, Z_2] \begin{Bmatrix} 1 \\ 0 \end{Bmatrix} \right)^2} \right) [r_1, r_2] \begin{Bmatrix} 1 \\ 0 \end{Bmatrix}
\end{aligned}
\tag{3.17}
$$

where r_1 and r_2 are the radii of each corresponding real node. The integration of the above integrals is made using the numerical Gauss integration method, see Dhatt and Touzout (1989). The assembly of different elementary integrals computed before is obtained as follows

$$
\mathbf{K}_{2,3} = \sum_{1}^{NelLD} (\mathbf{K}_e)_3 + (\mathbf{K}_e)_{3Z1} + (\mathbf{K}_e)_{3Z2} \tag{3.18}
$$

where $NelLD$ is the number of two node finite elements along the lined part.

The integral I_{e6} is written as follows for a finite element belonging to the left boundary

$$I_{e4} = [q_1, q_2](\mathbf{K}_e)_4^+(\mathbf{P}_{mn}^{I+})_{N_r} + [q_1, q_2](\mathbf{K}_e)_4^-(\mathbf{P}_{mn}^{I-})_{N_r}$$

$$(\mathbf{K}_e)_4^\pm = \begin{bmatrix} \cdots & [-\mathrm{i}k_{mn}^\pm(1+M_0^2) - kM_0] \int\limits_{-1}^{1} N_1(\xi) J_m\Big(\frac{\chi_{mn}}{a}r\Big)\frac{L_e}{2}r\,d\xi & \cdots \\ \cdots & [-\mathrm{i}k_{mn}^\pm(1+M_0^2) - kM_0] \int\limits_{-1}^{1} N_2(\xi) J_m\Big(\frac{\chi_{mn}}{a}r\Big)\frac{L_e}{2}r\,d\xi & \cdots \end{bmatrix}_{2N_r} \tag{3.19}$$

The integral I_{e5} is written as follows for an two-node finite element belonging to the right boundary

$$I_{e5} = [q_1, q_2](\mathbf{K}_e)_5^+(\mathbf{P}_{mn}^{II+})_{N_r} + [q_1, q_2](\mathbf{K}_e)_5^-(\mathbf{P}_{mn}^{II-})_{N_r}$$

$$(\mathbf{K}_e)_5^\pm = \begin{bmatrix} \cdots & [\mathrm{i}k_{mn}^\pm(1+M_0^2) - kM_0] \int\limits_{-1}^{1} N_1(\xi) J_m\Big(\frac{\chi_{mn}}{a}r\Big)\frac{L_e}{2}r\,d\xi & \cdots \\ \cdots & [\mathrm{i}k_{mn}^\pm(1+M_0^2) - kM_0] \int\limits_{-1}^{1} N_2(\xi) J_m\Big(\frac{\chi_{mn}}{a}r\Big)\frac{L_e}{2}r\,d\xi & \cdots \end{bmatrix}_{2N_r} \tag{3.20}$$

By using linear interpolation of the pressure, the integrals I_{e6} and I_{e7} are obtained as follows

$$\begin{aligned} I_{e6} &= (\mathbf{K}_e)_{61}\begin{Bmatrix} p_1 \\ p_2 \end{Bmatrix} + (\mathbf{K}_e)_{62}^+(\mathbf{P}_{mn}^{I+})_{N_r} + (\mathbf{K}_e)_{62}^-(\mathbf{P}_{mn}^{I-})_{N_r} \\ I_{e7} &= (\mathbf{K}_e)_{71}\begin{Bmatrix} p_1 \\ p_2 \end{Bmatrix} + (\mathbf{K}_e)_{72}^+(\mathbf{P}_{mn}^{II+})_{N_r} + (\mathbf{K}_e)_{72}^-(\mathbf{P}_{mn}^{II-})_{N_r} \\ (\mathbf{K}_e)_{61} = (\mathbf{K}_e)_{71} &= \begin{bmatrix} \vdots & \vdots \\ \int\limits_{-1}^{1} N_1(\xi) J_m\Big(\frac{\chi_{mn}}{a}r\Big)\frac{L_e}{2}r\,d\xi & \int\limits_{-1}^{1} N_2(\xi) J_m\Big(\frac{\chi_{mn}}{a}r\Big)\frac{L_e}{2}r\,d\xi \\ \vdots & \vdots \end{bmatrix}_{2N_r} \\ (\mathbf{K}_e)_{62}^+ = (\mathbf{K}_e)_{62}^- = (\mathbf{K}_e)_{72}^+ = (\mathbf{K}_e)_{72}^- &= \Bigg[\mathrm{diag}\Bigg(\int\limits_{-1}^{1} J_m\Big(\frac{\chi_m}{a}r\Big)^2\frac{L_e}{2}r\,d\xi\Bigg)\Bigg]_{N_r\times N_r} \end{aligned} \tag{3.21}$$

Once the elementary integrals are computed, the assembly of them is obtained as follows

$$\mathbf{K}_4^\pm = \sum_1^{NelL}(\mathbf{K}_e)_4^\pm \qquad \mathbf{K}_5^\pm = \sum_1^{NelR}(\mathbf{K}_e)_5^\pm \tag{3.22}$$

where $NelL$ and $NelR$ are, respectively, the number of two-node elements at the left and right boundaries

$$\begin{aligned} \mathbf{K}_{61} &= \sum_1^{NelL}(\mathbf{K}_e)_{61} \qquad & \mathbf{K}_{62}^\pm &= \sum_1^{NelL}(\mathbf{K}_e^\pm)_{61} \\ \mathbf{K}_{71} &= \sum_1^{NelR}(\mathbf{K}_e)_{71} \qquad & \mathbf{K}_{72}^\pm &= \sum_1^{NelR}(\mathbf{K}_e^\pm)_{72} \end{aligned} \tag{3.23}$$

The arrangement of the previous system leads to the following matrix system

$$\begin{bmatrix} \mathbf{K}_{M\times M} & (\mathbf{K}_4^-)_{M\times N_r} & (\mathbf{K}_4^+)_{M\times N_r} & (\mathbf{K}_5^-)_{M\times N_r} & (\mathbf{K}_5^+)_{M\times N_r} \\ (\mathbf{K}_{61})_{N_r\times M} & (\mathbf{K}_{62}^-)_{N_r\times N_r} & (\mathbf{K}_{62}^+)_{N_r\times N_r} & \mathbf{0} & \mathbf{0} \\ \mathbf{0} & \mathbf{0} & \mathbf{0} & \mathbf{0} & \mathbf{0} \\ \mathbf{0} & \mathbf{0} & \mathbf{0} & \mathbf{0} & \mathbf{0} \\ (\mathbf{K}_{71})_{N_r\times M} & \mathbf{0} & \mathbf{0} & (\mathbf{K}_{72}^-)_{N_r\times N_r} & (\mathbf{K}_{72}^+)_{N_r\times N_r} \end{bmatrix} \left\{ \begin{array}{c} \left\{ \begin{array}{c} p_1 \\ \vdots \\ p_M \end{array} \right\}_M \\ (\mathbf{P}_{mn}^{I-})_{N_r} \\ (\mathbf{P}_{mn}^{I+})_{N_r} \\ (\mathbf{P}_{mn}^{II-})_{N_r} \\ (\mathbf{P}_{mn}^{II+})_{N_r} \end{array} \right\} = \mathbf{0}$$

$$\mathbf{K}_{M\times M} = \mathbf{K}_1 + \mathbf{K}_{2,3} \tag{3.24}$$

with M is the number of nodes. For a given m, the azimuthal scattering matrix is defined as

$$\begin{Bmatrix} \mathbf{P}_{mn}^{I-} \\ \mathbf{P}_{mn}^{II+} \end{Bmatrix} = \mathbf{s}_{2N_r\times 2N_r} \begin{Bmatrix} \mathbf{P}_{mn}^{I+} \\ \mathbf{P}_{mn}^{II-} \end{Bmatrix} \tag{3.25}$$

This matrix is obtained by formulating the system of Eq. $(3.24)_1$ as follows

$$\mathbf{K}\mathbf{p} + \mathbf{A} \begin{Bmatrix} \mathbf{P}_{mn}^{I+} \\ \mathbf{P}_{mn}^{II-} \end{Bmatrix} + \mathbf{B} \begin{Bmatrix} \mathbf{P}_{mn}^{I-} \\ \mathbf{P}_{mn}^{II+} \end{Bmatrix} = \mathbf{0} \qquad \mathbf{C}\mathbf{p} + \mathbf{U} \begin{Bmatrix} \mathbf{P}_{mn}^{I+} \\ \mathbf{P}_{mn}^{II-} \end{Bmatrix} + \mathbf{V} \begin{Bmatrix} \mathbf{P}_{mn}^{I-} \\ \mathbf{P}_{mn}^{II+} \end{Bmatrix} = \mathbf{0} \tag{3.26}$$

where $\mathbf{p}$ is the nodal acoustic pressure vector, and the matrices $\mathbf{A}$, $\mathbf{B}$, $\mathbf{C}$, $\mathbf{U}$, and $\mathbf{V}$ are defined as

$$\begin{aligned} &\mathbf{A} = \Big[\mathbf{K}_4^- \mathbf{K}_5^+\Big] \qquad &&\mathbf{B} = \Big[\mathbf{K}_4^+ \mathbf{K}_5^-\Big] \qquad &&\mathbf{C} = \mathbf{K}_{61} + \mathbf{K}_{71} \\ &\mathbf{U} = \Big[\mathbf{K}_{62}^- \mathbf{K}_{72}^+\Big] \qquad &&\mathbf{V} = \Big[\mathbf{K}_{62}^+ \mathbf{K}_{72}^-\Big] \end{aligned} \tag{3.27}$$

The azimuthal scattering matrix is then written as

$$\mathbf{s} = (\mathbf{V} - \mathbf{C}\mathbf{K}^{-1}\mathbf{B}^{-1})(\mathbf{U} - \mathbf{C}\mathbf{K}^{-1}\mathbf{A}^{-1}) \tag{3.28}$$

The total scattering matrix of the studied duct $\mathbf{S}_{2N\times 2N}$ is obtained by repeating this operation for each m and by gathering the azimuthal matrices $\mathbf{s}_{2N_r\times 2N_r}$ and N is the total number of modes present in the duct.

4. Computation of the acoustic power attenuation

The axial acoustic intensity at a point $M(r,\theta,z)$ located in a plane section of the duct is given by Ville and Foucart (2003)

$$I_z(r,\theta,z) = \frac{1}{2}(1+M_0^2)\mathrm{Re}(P,V_z^*) + \frac{\rho_0, V_0}{2}\mathrm{Re}(V_zV_z^*) + \frac{V_0}{2\rho_0 c_0^2}(PP^*) \tag{4.1}$$

where V_z is the axial acoustic velocity and P is the acoustic pressure. The acoustic power is given by

$$W(z) = \sum_{m=-\infty}^{+\infty} \sum_{n=0}^{\infty} I_{z,mn}(z) N_{mn} \tag{4.2}$$

with N_{mn} is the normalization coefficient associated with the (m,n) mode defined as

$$N_{mn} = SJ_m^2(\chi_{mn})\Big(1 - \frac{m^2}{\chi_{mn}^2}\Big) \tag{4.3}$$

where $S = \pi a^2$ is the plane section are of the duct.

The axial acoustic intensity associated with the (m,n) mode $I_{z,mn}$ is given by the following expression in function of modal acoustic pressures and velocities

$$I_{z,mn}(z)=\frac{1}{2}(1+M_0^2)\mathrm{Re}(P_{mn}V_{z,mn}^*)+\frac{\rho_0V_0}{2}\mathrm{Re}(V_{z,mn}V_{z,mn}^*)+\frac{V_0}{2\rho_0c_0^2}\mathrm{Re}(P_{mn}P_{mn}^*) \tag{4.4}$$

From this expression, the incident, reflected, transmitted and retrograde modal intensities are given by

$$\begin{aligned}
I_{z,mn}^{I+}&=\frac{(1+M_0^2)N_{mn}k_{mn}^+}{2\rho_0c_0(k-M_0k_{mn}^+)}|P_{mn}^{I+}|^2 \qquad & I_{z,mn}^{I-}&=\frac{(1+M_0^2)N_{mn}k_{mn}^-}{2\rho_0c_0(k-M_0k_{mn}^-)}|P_{mn}^{I-}|^2\\
I_{z,mn}^{II+}&=\frac{(1+M_0^2)N_{mn}k_{mn}^+}{2\rho_0c_0(k-M_0k_{mn}^+)}|P_{mn}^{II+}|^2 \qquad & I_{z,mn}^{II-}&=\frac{(1+M_0^2)N_{mn}k_{mn}^-}{2\rho_0c_0(k-M_0k_{mn}^-)}|P_{mn}^{II-}|^2
\end{aligned} \tag{4.5}$$

The acoustic power attenuation W_{att} of a two-port duct is defined as the ratio between the acoustic power of incoming pressures from the two sides of the duct W^{in} and the acoustic power of out-coming pressures from the two sides of the duct W^{out}

$$\begin{aligned}
W_{att}(dB)&=10\log\frac{W^{in}}{W^{out}}\\
W^{in}&=\sum_{m=-P}^{P}\sum_{n=0}^{Q}\frac{(1+M_0^2)N_{mn}}{2\rho_0c_0}\Big(\frac{k_{mn}^+}{k-M_0k_{mn}^+}|P_{mn}^{I+}|^2+\frac{k_{mn}^-}{k-M_0k_{mn}^-}|P_{mn}^{II-}|^2\Big)\\
W^{out}&=\sum_{m=-P}^{P}\sum_{n=0}^{Q}\frac{(1+M_0^2)N_{mn}}{2\rho_0c_0}\Big(\frac{k_{mn}^-}{k-M_0k_{mn}^-}|P_{mn}^{I-}|^2+\frac{k_{mn}^+}{k-M_0k_{mn}^+}|P_{mn}^{II+}|^2\Big)
\end{aligned} \tag{4.6}$$

The acoustic power attenuation is then written as follows

$$W_{att}(dB)=10\log\frac{W^{in}}{W^{out}}=10\log\frac{\sum_{i=1}^{2N}|d_i|^2}{\sum_{i=1}^{2N}\lambda_i|d_i|^2} \tag{4.7}$$

where λ_i are the eigenvalues of $\mathbf{H}$ defined as

$$\begin{aligned}
\mathbf{H}_{2N\times2N}&=\Big[[\,\mathrm{diag}\,(XO)]_{2N\times2N}\mathbf{S}_{2N\times2N}[\,\mathrm{diag}\,(XI)]_{2N\times2N}^{-1}\Big]_{2N\times2N}^{\mathrm{T}*}\\
&\quad\cdot\Big[[\,\mathrm{diag}\,(XO)]_{2N\times2N}\mathbf{S}_{2N\times2N}[\,\mathrm{diag}\,(XI)]_{2N\times2N}^{-1}\Big]_{2N\times2N}\\
XI_{mn}&=\sqrt{\frac{N_{mn}}{2\rho_0c_0}\Big(\frac{(1+M_0^2)k_{mn}^+}{k-M_0k_{mn}^+}+\frac{k_{mn}^+M_0}{(k-M_0k_{mn}^+)^2}+M_0\Big)}\\
XO_{mn}&=\sqrt{\frac{N_{mn}}{2\rho_0c_0}\Big(\frac{(1+M_0^2)k_{mn}^-}{k-M_0k_{mn}^-}+\frac{k_{mn}^-M_0}{(k-M_0k_{mn}^-)^2}+M_0\Big)}\\
\mathbf{d}_{2N}&=\mathbf{U}_{2N\times2N}^{\mathrm{T}*}(\mathbf{\Pi}^{in})_{2N}
\end{aligned} \tag{4.8}$$

with $\mathbf{U}$ is the eigenvector matrix of $\mathbf{H}$ and $\mathrm{T}*$ denotes conjugate transpose.

5. Numerical results

5.1. Scattering matrix coefficients

The studied duct in this paper is a 1 meter long cylindrical duct composed of three parts: 0.35 m rigid wall duct, 0.3 lined duct and 0.35 m rigid wall duct. This duct is similar to the experimental duct used by Taktak *et al.* (2010). The computation of the multimodal scattering matrix and the acoustic power attenuation is made by supposing that the duct is lined by a Helmholtz resonator composed of a perforated plate with the thickness $e = 0.8\,\mathrm{mm}$, the hole diameter $d = 1\,\mathrm{mm}$ with a perforation ratio $\sigma = 5\%$ of the honey comb structure with thickness $D = 20\,\mathrm{mm}$ and a rigid wall plate. This kind of liner is characterized by its acoustic impedance Z. In the present work, the acoustic impedance model of Elnady and Boden (2003) is used as the input for computation of the numerical multimodal scattering matrix and the acoustic power attenuation of the studied duct. This model gives the resonance frequency at $ka = 2.22$. Computations are made for different Mach numbers ($M_0 = 0,\ 0.1,\ 0.2$) over the frequency band $ka \in [0, 3.8]$ to evaluate the flow effect.

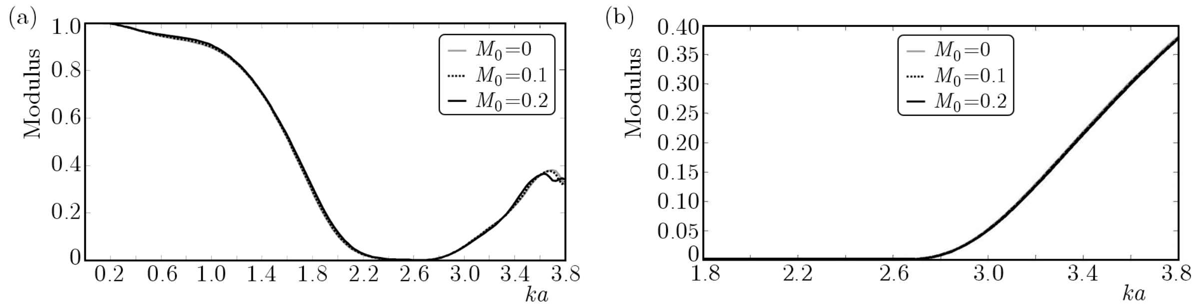

Fig. 2. Modulus of the transmission coefficients $T^+_{00,00}$ (a) and $T^+_{10,10}$ (b) versus ka for several Mach numbers

Figures 2a,b present the moduli of transmission coefficients $T^+_{00,00}$ and $T^+_{10,10}$ computed in the same direction of the flow versus of the nondimensional wave number ka for different Mach numbers. The modulus of the coefficient $T^+_{00,00}$ shows that it is near 1 in $ka \in [0, 0.8]$. From $ka = 0.8$, this modulus decreases with the frequency until becoming nil in the interval $ka \in [2.4, 2.8]$ near the theoretical resonance frequency. Then, an increase of the modulus is observed in the rest of the studied frequency band until reaching 0.4 at $ka = 3.8$. For the $T^+_{10,10}$ modulus, an increase versus ka is observed from $ka = 2.8$ to reach 0.4 at $ka = 3.8$. Figures 2a,b also show that there are no significant effects of the flow on transmission coefficients. Figures 3a,b,c present, respectively, the moduli of reflection coefficients $R^+_{00,00}$, $R^+_{10,10}$ and $R^+_{20,20}$

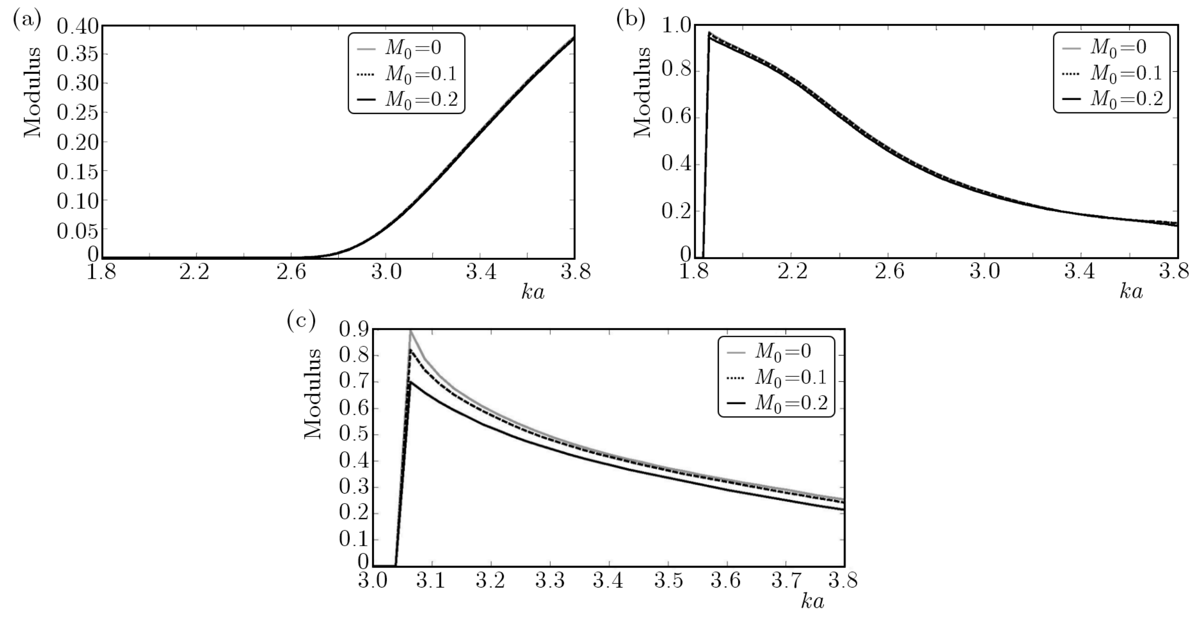

Fig. 3. Modulus of the reflection coefficients $R^+_{00,00}$ (a), $R^+_{10,10}$ (b) and $R^+_{20,20}$ (c) versus ka for several Mach numbers

of the studied duct. Oscillations are observed on the reflection coefficient $R^+_{00,00}$. The reflection coefficients of higher order modes are close to 1 near the cut on frequencies, then a decrease of their moduli is observed versus ka. Figures 3a,b,c show the flow effects on reflection coefficients: when the flow velocity increases, the reflection coefficients moduli decrease except the $R^+_{00,00}$ coefficient modulus in $ka \in [1.2, 1.8]$. This decrease is more apparent on the $(0,0)$ mode reflection coefficient (~ 0.05) and $(2,0)$ mode (~ 0.2) and less important than the $(1,0)$ mode.

5.2. Acoustic power attenuation

Acoustic power attenuations are computed using a configuration of unit modal incident pressures from one side of the duct (left) and in the same direction of flow, see Taktak *et al.* (2010) ($\mathbf{P}^{in} = [1,1,1,1,1,0,0,0,0,0]^{\mathrm{T}}$). Figures 4a,b,c present the acoustic power attenuation of the studied duct versus ka, respectively, in presence of $(0,0)$, $(1,0)$, $(2,0)$ for different studied Mach numbers. They show that attenuations are dependent of the incident wave and that the maximum of attenuation is observed near the liner resonance frequency. The amplitude and the frequency of this maximum is dependent on the flow speed. Figure 4a shows that this maximum is equal to 15 dB without flow at $ka = 3.1$, 17 dB for $M_0 = 0.1$ at $ka = 3$ and 19 dB for $M_0 = 0.2$ at $ka = 2.95$. The same remark is observed in presence of the $(1,0)$ and $(2,0)$ mode: without flow, the maximum of attenuation in presence of the $(1,0)$ is 12 dB at $ka = 3.2$, 13 dB at $ka = 3.1$ for $M_0 = 0.1$ and 14 dB at $ka = 3.05$ for $M_0 = 0.2$. These figures allowed concluding that an increase in the flow velocity generates a increase in the acoustic power attenuation and a decrease in the maximum of attenuation frequency.

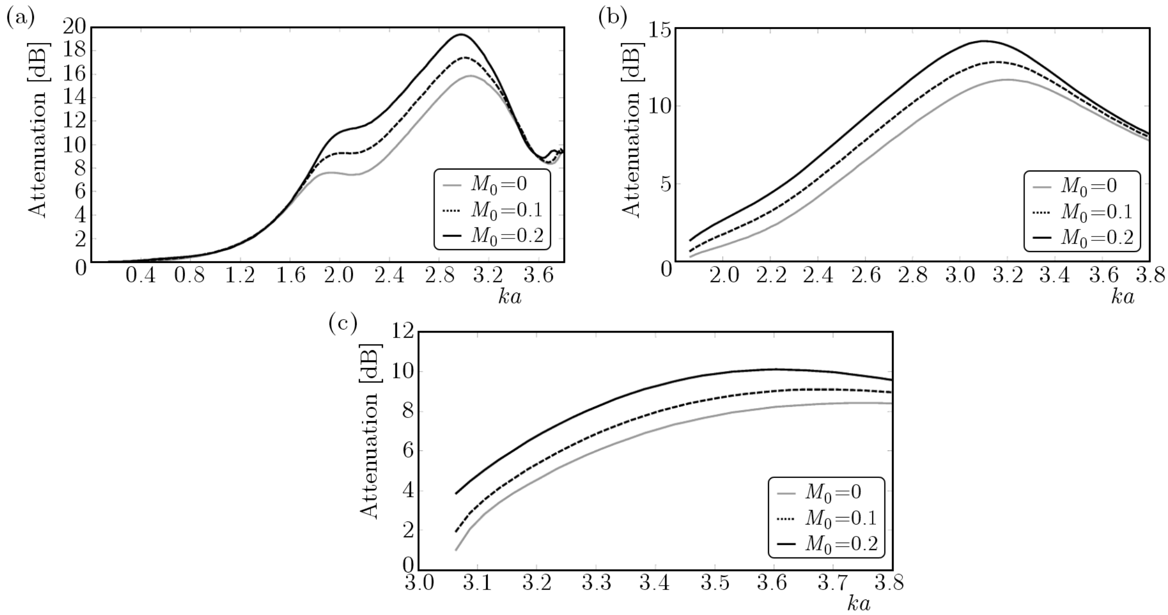

Fig. 4. Acoustic power attenuation of the studied duct in the presence of $(0,0)$ mode (a), $(1,0)$ mode (b) and $(2,0)$ mode (c) versus ka for several Mach numbers

6. Conclusions

In this study, a numerical method for the characterization of a lined duct inthe presence of flow was developed and presented. This method is based on the computation of the multimodal scattering matrix as well as the acoustic power attenuation. By varying the flow velocity, its effect was evaluated: the increase of the flow decreases the reflection coefficients when the effect is weak on the transmission coefficients. For the acoustic power attenuation, the increase of the flow velocity increases the attenuation and decreases the frequency of the maximum attenuation.

Acknowledgements

This work was carried out in the framework of Tunisian-French research project DGRSRT/CNRS 09/R 11-43 on the modeling of the vibro-acoustic problems.

References

1. Abom M., 1991, Measurement of the scattering matrix of acoustical two-ports, *Mechanical Systems Signal Processing*, **5**, 2, 89-104
2. Akoum M., Ville J.M., 1998, Measurement of reflection matrix of a discontinuity in a duct, *Journal of the Acoustical Society of America*, **103**, 5, 2463-2468
3. Aurégan Y., Starobinski R., 1998, Determination of acoustical energy dissipation/production potentiality from the acoustic transfer functions of a multiport, *Acta Acustica United with Acustica*, **85**, 788-792
4. Bi W.P., Pagneux V., Lafarge D., Aurégan Y., 2006, Modelling of sound propagation in non-uniform lined duct using a Multi-Modal Propagation Method, *Journal of Sound and Vibration*, **289**, 1091-1111
5. Craggs, A., 1989, The application of the scattering matrix and matrix condensation methods with finite elements to ducts acoustics, *Journal of Sound and Vibration*, **132**, 2, 393-402
6. Dhatt G., Touzot G., 1989, *Presentation of the Finite Element Method*, Maloine S.A. Editeur, Paris
7. Elnady T., Bodén H., 2003, On semi-empirical liner impedance modeling with grazing flow, *AIAA Paper*, **2003-3304**
8. Leroux M., Job S., Aurégan Y., Pagneux V., 2003, Acoustical propagation in lined duct with flow. Numerical simulations and measurements, *10th International Congress of Sound and Vibration*, Stockholm, Sweden, 3255-3262
9. Lesueur L., 1988, *Rayonnement acoustique des structures: Vibroacoustique et Interactions Fluide Structure*, Editions Eyrolles, Paris
10. Lung T.Y., Doige A.G., 1983, A time-averaging transient testing method for acoustic properties of piping systems and mufflers with flow, *Journal of the Acoustical Society of America*, **73**, 867-876
11. Munjal M.L., 1987, *Acoustics of Ducts and Mufflers*, Wiley-Interscience, New York
12. Peat K.S., 1988, The transfer matrix of a uniform duct with a linear temperature gradient, *Journal of Sound and Vibration*, **123**, 1, 43-53
13. Pierce A.D., 1981, *Acoustics: An Introduction to its Physical Principles and Applications*, McGraw-Hill, New York
14. Sitel A., Ville J.M., Foucart F., 2003, An experimental facility for measurement of acoustic transmission matrix and acoustic power dissipation of a duct discontinuity in higher modes propagation conditions, *Acta Acustica United with Acustica*, **89**, 586-594
15. Sitel A., Ville J.M., Foucart F., 2006, Multimodal procedure to measure the acoustic scattering matrix of a duct discontinuity for higher order mode propagation conditions, *Journal of the Acoustical Society of America*, **120**, 5, 2478-2490
16. Taktak M., Ville J.M., Haddar M., Gabard G., Foucart F., 2010, An indirect method for the characterization of locally reacting liners, *Journal of the Acoustical Society of America*, **127**, 6, 3548-3559

17. To C.W.S., Doige A.G., 1979, A transient testing technique for the determination of matrix parameters of acoustic systems, I: Theory and principles, *Journal of Sound and Vibration*, **62**, 207-222

18. To C.W. S., Doige A.G., 1979, A transient testing technique for the determination of matrix parameters of acoustic systems, II: Experimental procedures and results, *Journal of Sound and Vibration*, **62**, 223-233

19. Ville J.M., Foucart F., 2003, Experimental set up for measurement of acoustic power dissipation in lined ducts for higher order modes propagation with air mean flow conditions, *Journal of the Acoustical Society of America*, **114**, 4, 1742-1748

Numeryczna charakteryzacja wyściełanego przewodu osiowo-symetrycznego z przepływem za pomocą wielomodalnej macierzy rozpraszania

Streszczenie

W pracy zaprezentowano numeryczną metodę wyznaczania macierzy rozpraszania dla wyściełanego przewodu z uwzględnieniem wewnętrznego przepływu czynnika. Metodę oparto na zastosowaniu równania konwekcji Helmholtza z wprowadzeniem ciśnień modalnych na brzegach jako dodatkowych stopni swobody układu. Efekty brzegowe na wlocie i wylocie przewodu falowego o skończonej długości pominięto. Wybór macierzy rozpraszania uzasadniono faktem, że reprezentuje ona wewnętrzną charakterystykę analizowanego modelu. Zaproponowany element skończony zweryfikowano poprzez porównanie z istniejącymi rozwiązaniami analitycznymi dla prostych przypadków konfiguracji przewodu. Następnie numerycznie obliczono wartości elementów macierzy rozpraszania oraz współczynniki tłumienia akustycznego dla kilku prędkości przepływu w celu określenia, jak dalece wpływa on na badany układ.

Manuscript received March 9, 2012; accepted for print June 14, 2012